

# Stability Analysis of Magneto-Rheological Damper for Suspension of Commercial Vehicles

Rupesh Kumar Patnaik, N Tamarasan



**Abstract:** This paper aims at improving the efficiency of magneto-rheological dampers, which utilizes a smart material in the form of magneto-rheological fluid, over the typical-build conventional dampers. The proposed design has been modeled for its implementation in commercial vehicles which extensively relies on conventional shock-absorbers for the safety and comfort of its occupants, considering the space available for mounting the system. Dimensional constraints based on commercial vehicles pertaining to the hatchback segment have been taken in COMSOL® and analyzed to generate a considerable amount of damping force for realizable inputs. As the analysis requires a profound consideration of highly coupled physics interface, COMSOL® Multi-physics is chosen as the relevant platform which makes it suitable to fulfill the criteria at hand. The damping forces achieved in the model are determined based on the linear Bingham model and the non-linear hysteretic Bouc-Wen model. A rigorous analysis was conducted to realize the variation in damping force values on account of the hysteresis losses induced in the system. Optimization based on Taguchi's mixed level design approach is used to attain the optimal design parameters of MR damper. MRF-140 CG fabricated by Lord Corporation is adopted to introduce the rheological effect of MR fluid on the proposed model.

**Index Terms:** Bingham model, Bouc-Wen model, COMSOL, damping force, Magneto - Rheological damper.

## I. INTRODUCTION

The usage of smart materials in the prevailing scenario of today's automotive industries has been spearheading the entire sector to a whole new level. The range of applications they possess remains unparalleled, one of which is in the field of suspension systems pertaining to the automotive sector. These systems employ certain smart fluids as a substitute to the conventional fluids which produces highly pronounced effect in a more effective way. For today's luxurious and lavish era, the positive consequence of using a magneto-rheological damper in lieu of mostly used conventional dampers in vehicles leads to its instant response time of

approx. 0.02 seconds, variation of its viscosity in few milliseconds, the ease to construct, need of very meager operational power and more capability to absorb vibration. This paper intends to develop an original design of MR damper for a commercial vehicle of hatchback type that can successfully replace the conventional damper already inherent in the vehicle and also provides a reasonable approach of optimizing the geometric dimensions with the aid of statistical tool namely Taguchi's method as conducted by Ashwani and Mangal [1]-[2]. They built an axisymmetric 2-D model of MR damper based on finite element techniques and evaluated the damping force for the proposed model. Krishnan Unni R. and Tamarasan N. [3] devised a model to replace the traditional damper assembly with a fully controllable device employing magneto-rheological dampers and fabricated the same to be used in All Terrain Vehicles (ATV). A rigorous analysis regarding the application of magneto-rheological fluid in the braking system of an All-Terrain Vehicle (ATV) was performed by Luckachan K. George et al. [4] employing Linear Bingham model and Herschel-Bulkley model. Coupled physics analysis was carried out in COMSOL® software wherein the braking torque of the proposed model was calculated efficiently. M. Zapateiro et al. [5] studied the non-linear hysteretic response of MR dampers and put forward a control strategy to mitigate any vibration in smart structures (buildings) in the face of calamities such as earthquakes. They put forward a proposition regarding the stability of a building without ground support equipped with a magneto-rheological damper when triggered by a seismic signal. N.M. Kwok et al. [6] suggested an asymmetrical parametric model for MR dampers. The parameters for the proposed model were recognized using Genetic Algorithm (GA) which is economical both in terms of computational time and cost. Adopting this technique, they enhanced the adaptability of the proposed algorithm by dissolving the selection stage onto the crossover and mutation operations. In [7], the parameters were identified by a GA which uses the resulting model for vibration control in vehicles. One of the fundamental objectives of this paper is to augment the efficiency of the proposed model without any compromise in performance of the magneto-rheological effect. Concerning this, one of the critical parameters which need keen consideration is the damping effect set up by the damper situated next to the spring assembly.

Revised Manuscript Received on October 30, 2019.

\* Correspondence Author

**Rupesh Kumar Patnaik\***, PG Student, Department of Mechanical Engineering, Amrita School of Engineering, Coimbatore, Amrita Vishwa Vidyapeetham, India.

**N Tamarasan**, Assistant Professor, Department of Mechanical Engineering, Amrita School of Engineering, Coimbatore, Amrita Vishwa Vidyapeetham, India.

© The Authors. Published by Blue Eyes Intelligence Engineering and Sciences Publication (BEIESP). This is an [open access](http://creativecommons.org/licenses/by-nc-nd/4.0/) article under the CC BY-NC-ND license (<http://creativecommons.org/licenses/by-nc-nd/4.0/>)

A. Smart materials

Basically, they are the engineered materials that have

one or more characteristics which can be fundamentally altered in a contained way by extrinsic inducements viz. light, temperature, mechanical deformations, electric or magnetic excitations, etc., which greatly influences its behavior. All the variations are markedly reversible, in other words, the materials subsequently return to their initial states once the effect of the external stimulus kicks off. Different classes of smart materials are available, each showcasing interestingly unique properties which can be exploited in highly complicated real-world situations. Some of these include shape memory alloys (SMA), piezoelectric materials, magnetostrictive materials, thermochromic materials, ferro fluids, smart fluids, etc. The magneto-rheological fluid is one such classic fluid which makes its use in different automotive applications, more particularly in suspension systems.

B. Magneto-rheological (MR) fluids

A magneto-rheological fluid falls under the category of smart fluid, which usually is composed of oil (such as kerosene, silicone oil, etc.) in which micron-sized iron particles are suspended throughout. Jacob Rabinow [8], in the late 1940s, can be fundamentally credited as the pioneer for his discovery of MR fluids at its infancy and its subsequent development at a later stage (1948, 1951). R. Jolly et al. [9] examined the magnetic and rheological behavior of various commercially available MR fluids based on typical design criteria. Based on their properties, they were assigned a certain figure of merit which decides the applicability of the fluid in the real-world scenarios. When the field is activated, the iron granules becomes instantly smart, thereby organizing themselves in a linear fashion throughout the magnetic flux lines as depicted in figure 1. As a result, due to this effect, the fluid’s viscosity increases to the extent that it becomes a viscoelastic solid. This property of the fluid in transforming from liquid to semi-solid state makes it extremely valuable [10] to be used in suspension systems. In other words, they accomplish the desired objective by altering the system’s properties in a desirable manner. The application of these fluids are widely employed to actively regulate the vibration & motion of several components of an automobile, namely, engine mount, shock absorbers, seat dampers, braking systems, etc.

C. Mathematical models of MR damper

Various parametric models viz. Bingham, Dahl, LuGre and Bouc-Wen have been developed which can effectively describe the non-linear effects characterized by the system and hence, is a field of massive interest as more and more researchers are probing to refine these recognized models which can still acquire more pronounced results. Two models viz. the Bingham and the Bouc-Wen model have been considered in this analysis. The former is a basic linear model while the latter is an evolutionary paradigm which can precisely predict the non-linear nature of the system.

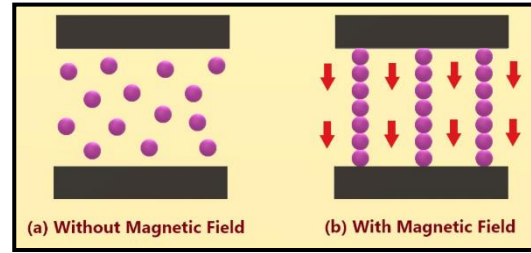


Fig. 1. Action Of Iron Granules in The Presence Of Magnetic Field

a. Bingham model

The greatest nobility of rheological fluids is the shear yield stress and acquires this behavior arising out of the highly Non-Newtonian nature of such fluids. The MR fluid follows the attributes of certain class of Non-Newtonian fluid called Bingham fluid which does not show any change in shear rate until considerable stress has been attained, causing the fluid to act predominantly as a quasi-solid rather than a viscous flowing liquid, as shown in figure 2. That particular value of the shear stress corresponding to zero amount of shear rate is known as yield stress of the fluid which largely relies on the intensity of magnetic field induced to the fluid.

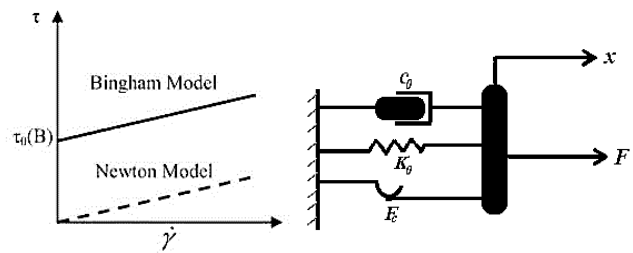


Fig. 2. Illustration of Bingham model

Among several parametric models available, one of the earlier models is the Bingham viscoplastic model proposed by Stanway et al. [11] where a Coulomb friction element ( $F_c$ ) is arranged in parallel configuration with a viscous damping element. The Bingham model depicted in figure 3 is defined by the following linear equation as,

$$F = F_c \text{sgn}(\dot{x}) + c_0 \dot{x} + K_0 x \tag{1}$$

Where  $x$  and  $\dot{x}$  are the relative displacement and velocity of the piston respectively,  $F_c$  is controller frictional force,  $c_0$  is damping coefficient,  $K_0$  is stiffness of spring. The signum function  $\text{sgn}(\dot{x})$  takes into account the direction of the frictional force  $F_c$  w.r.t. the relative velocity ( $\dot{x}$ ).

b. Bouc-Wen model

This parametric model by virtue of its adaptability and simplicity has been widely utilized in many systems involving hysteresis behavior. It was initially implemented by Bouc [12] in 1967, but it was Wen [13] who pursued the interpretation of this model by generating an array of hysteretic shapes.



The magnetorheological damper equipped with the hysteretic model consists of stiffness, passive damper and hysteresis loop components. The graphical representation of the Bouc-Wen model is illustrated in figure 4 which has a time-dependent variable  $z$  that actively captures the dynamic response efficiently. This model proposed by Wen can accurately characterize the relationship between applied force and displacement developed by the damper and can generate the force-velocity hysteretic loop more closely to the actual response.

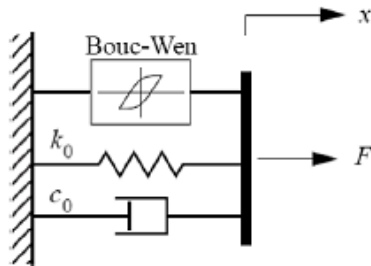


**Fig. 4. Schematic Illustration Of Bouc-Wen Model**

The damping force  $F$  produced by the system as proposed by Spencer et al. [14] is given by

$$F = k_0(x - x_0) + c_0\dot{x} + \alpha z \quad (2)$$

Where the time-transformative parameter  $z$  is given by the following expression

$$z = -|\dot{x}||z||z|^{n-1} - \beta\dot{x}|z|^n + A\dot{x} \quad (3)$$

Here,  $x$  represents the linear displacement of piston rod,  $x_0$  is the damping coefficient which is taken as a constant,  $\alpha$  denotes the coefficient predicted by the control system and the dynamics of magnetorheological fluid. The parameter  $z$  can evolve from a sinusoidal to a pseudo-rectangular function of time relying on the parameters  $\gamma$ ,  $\beta$  and  $A$ . These parameters maintain the linearity while discharging and evenness of the transformation from elastic to the plastic domain. In the proposed model, the variables  $c_0$  and  $\alpha$  possesses a linear functional dependency with the control voltage  $u$ .

## II. METHODOLOGY

The performance of suspension systems in an automobile is acutely vital pertaining to the safety, ride and comfort of the occupants irrespective of the class of the vehicle under consideration. Owing to the fact that suspension systems play an indispensable role in the effective functioning of the vehicle, the existing conventional systems can be further fine-tuned with the usage of MR dampers. In this regard, MR dampers have proven its worth in terms of quality of ride, substantial improvement in efficiency as a result of reduced shocks and vibrations thereby enhancing the safety and comfort of the passengers. Thus, a significant amount of research has already begun in this field and yet remains much to be explored. With the aid of Finite Element Methods (FEM), various facets of design in terms of geometry, selection of feasible materials, improvement in damping force, etc. can be probed.

The efficiency of MR dampers can be substantially improved by adopting either one or a combination of the following parameters:

- By developing a new design by modifying the dimensions such as the diameter of the cylinder, the thickness of MR fluid gap, etc.
- By changing the MR fluid itself,
- By predicting the exact behavior of the system to include the effects of temperature and other physical factors by incorporating certain models such as the Bingham, Herschel - Bulkley, Bouc - Wen, etc.

For the purpose of understanding the dynamics of magnetorheological damper, it becomes essential to conduct a static analysis. First and foremost task is to create a model which is symmetric to the axis of the damper suited for use in hatchback segment of commercial vehicles (CV). For different classes and body styles of commercial vehicles, the space available for practically mounting the damper varies more or less to a small extent. Yet it is essential to estimate the approximate space available for its installation from an implementation point of view as one of the objectives demand these dampers to eventually replace the conventional ones without compromising the damping force developed by the MR damper. So, based on the spatial requirements, the ranges for different dimensional parameters were established as shown in Table I. Optimization was carried out to obtain the preferred feasible values which would then be useful for creating the 2-D model using COMSOL®. The 2-D geometry of the damper is illustrated in figure 5.

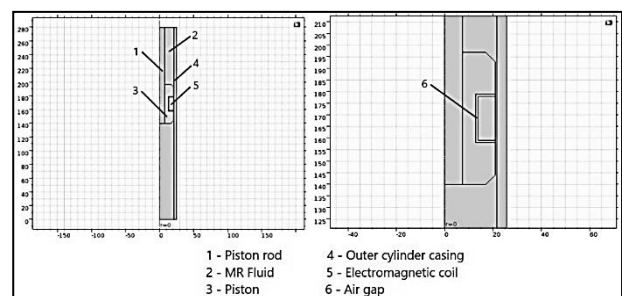


**Fig. 5. Schematic illustration of MR damper depicting its various components and an enlarged view of piston (right portion).**

Basic domains required for the analysis of MR damper includes the outer cylinder, piston, piston rod, MR fluid working gap, electromagnetic coil and the air gap.

### A. Dimensions

Owing to the symmetrical shape of the damper, a 2-D axisymmetric model was created using the COMSOL's geometry interface. Adopting an axisymmetric approach serves in reducing a considerable load of computational time and power which greatly simplifies the problem. The dimensional constraints were determined based on the longitudinal distance between the mounting points located on the chassis and the wheel axis. The circumferential area which would determine the maximum diameter constraint for the cylinder outer casing was



also taken into consideration. Owing to the practical measurements carried out on a typical hatchback, the distance between the rubber mountings were calculated as 310 mm and the maximum diameter available for the installation of the damper was found out to be 56 mm. Based on the longitudinal dimensions available for the installation of the damper in a typical hatchback model, the geometrical parameters were determined. The overall length of the damper (cylinder) was taken as 280 mm. Also, based on the neighboring spatial dimensions, the outer diameter of the cylinder was determined as 51.4 mm. Preserving an aspect ratio between the cylinder and piston dimensions, the length and diameter of the piston was estimated to be 57 mm and 42 mm respectively. The outer thickness of cylinder casing, the width of the coil, fluid gap thickness, pole length and distance between poles were taken in their respective ranges and final dimensions were evaluated based on the optimization scheme presented in the following section.

**Table I. Ranges of various parameters of MR damper.**

Parameter of MR damper	Dimensional range (mm)
Coil width	6-9
Fluid gap	0.7-1
Casing thickness	3-6
Pole length	15-18
Distance between poles	17-20

A chamfer of 4 mm from the vertex was given on the upper and lower periphery of the piston which reduces the material, thereby weight of the piston without much effect on the field interaction with the fluid. Consequently, overall weight of the damper also lowers which has a positive influence on the performance of a vehicle's suspension system. As the MR fluid contains tiny granules of ferrous particles, the proposed model can be designed to scrutinize the effect of the fluid along the fluid working gap or even on the piston of the damper to evaluate the pressure distribution of the fluid on that particular area. As the subject under consideration requires the conversion of energy from electrical to magnetic to mechanical pathway, it becomes a highly coupled problem, the analysis of which necessitates a Multiphysics approach. Developing a Multiphysics model also enable us to calculate the effective damping force across the MR working gap effectively.

*a. Optimization*

For the purpose of achieving the desired damping force based on certain restraints imposed on the dimensions of the proposed model, it is essential to perform an optimization of parameters. By mere inspection, it is obvious that the damping force primarily depends on five crucial parameters viz. width of the coil (D), pole length (L), the distance between poles (l), MR working gap (h) and casing thickness (t).

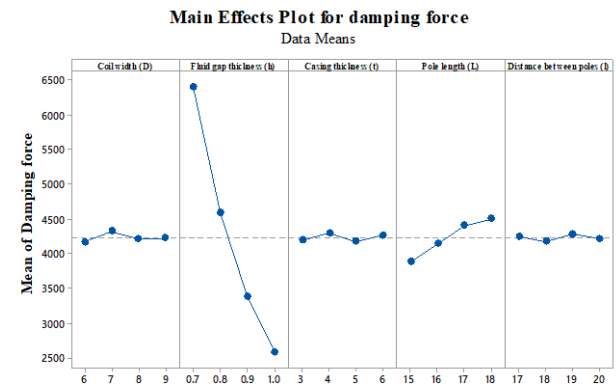
Optimization based on Taguchi mixed level design concept was carried out using an L16 orthogonal array. For this particular analysis, the maximum allowable current supplied to the coil is limited to 2A and a parametric test of sixteen distinct models was conducted and damping forces were evaluated using COMSOL® Multiphysics. Piston velocity of 1.24m.s<sup>-1</sup> is considered for the purpose of simulation. Table II shows various damping force values for the designed models.

**Table II. Optimization array depicting the damping force values.**

Coil width (D)	Fluid thickness (h)	Cylinder thickness (t)	Pole length (L)	Distance between poles (l)	Damping force (N)
6	0.7	3	15	17	5965.32
6	0.8	4	16	18	4447.59
6	0.9	5	17	19	3474.96
6	1	6	18	20	2807.06
7	0.7	4	17	20	6708.96
7	0.8	3	18	19	4654.59
7	0.9	6	15	18	3097.49
7	1	5	16	17	2540.31
8	0.7	5	18	18	6529.88
8	0.8	6	17	17	4789.72
8	0.9	3	16	20	3221.07
8	1	4	15	19	2335.37
9	0.7	6	16	19	6387.83
9	0.8	5	15	20	4154.12
9	0.9	4	18	17	3712.28
9	1	3	17	18	2651.30

\* All input variables are in mm.

From the optimization array, the maximum force developed by the damper is 6708.96 N and the corresponding set of values are: D = 7 mm, h = 0.7 mm, t = 4 mm, L = 17 mm and l = 20 mm.



Means: Larger is better.

**Fig. 6. Comparison Of Critical Parameters With Mean Of The Response Variable**

From the above plot, it can be seen that two parameters viz. pole length (L) and distance between poles (l) seems to vary when compared with the values already found. Hence, the optimized parameters were again re-evaluated and found out to be:

**Table III. Optimized Values After Re-Evaluation.**

Coil width (D)	Fluid thickness (h)	Cylinder thickness (t)	Pole length (L)	Distance between poles (l)	Damping force (N)
7	0.7	4	18	19	7402.61

The response table for means was predicted using Taguchi's analysis. It is evidently clear from the response table that fluid gap thickness and pole length have the maximum influence on the response variable characteristic i.e. damping force values as compared to



other parameters. Thus for better clarification, a surface plot was generated between these 3 variables as shown in figure 7. In this plot, the response variable (in this context, the damping force,  $F$ ) is represented by a continuous surface on z-axis while the critical parameters namely, pole length ( $L$ ) and MR fluid gap thickness ( $h$ ) are represented on x- and y-axes respectively.

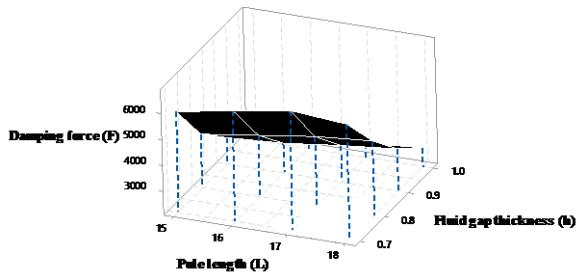


**Fig. 7. Surface Plot Of Damping Force Versus Fluid Gap Thickness And Pole Length**

The final optimized design dimensions for the proposed model are presented in Table IV.

**Table IV. Final Optimized Dimensions For Design Of MR Damper.**

Parameter of MR damper	Dimensions (mm)
Radius of piston rod ( $r$ )	7.5
Radial distance from piston rod to coil ( $H$ )	6.5
Cylinder thickness ( $t$ )	4
Piston radius ( $R$ )	21
Axial distance between the two poles ( $l$ )	19
Pole length ( $L$ )	18
Fluid working gap ( $h$ )	0.7
Width of coil ( $D$ )	7

**B. Material selection**

Taking the optimized design into consideration, the relevant materials designated for the model largely rely on the magnetic properties of the fluid viz. relative permeability and permittivity analogous with properties of the fluid. For obtaining a highly distributed magnetic flux which would achieve uniform damping force, materials bearing high relative permeability values are selected. Befitting this condition, AISI 4340 is chosen as the material for piston, piston shaft and cylinder which has a density of  $7850\text{kg}\cdot\text{m}^{-3}$  approx.). Copper being highly conductive is chosen as the material for the electromagnetic coil and is assigned along the boundary of the coil. A major part of the analysis has been focused only on the fluid gap along the periphery of the piston where the interaction between the fluid and the piston head over which the coil is wound is likely to happen. Hence, the fluid properties are designated to the domain that is fixed amidst the periphery of the piston and the external cylinder.

The key parameter which greatly influences their selection is the fluid’s yield stress. Apparently, it ensures that MR fluids possess a significantly higher value of yield stress than ER fluids. Besides, evident from the fact that the dampers are liable to operate at extreme climatic conditions, MR fluids

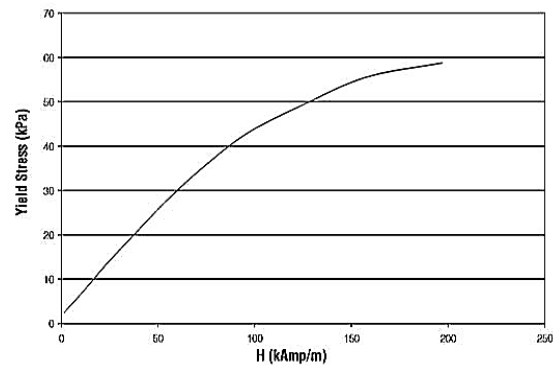
fulfill the criteria as they have a broad temperature range of operation spanning from minus  $40\text{ }^\circ\text{C}$  to  $150\text{ }^\circ\text{C}$ . Thus, such materials designated to each particular domain in COMSOL® Multiphysics are systematically illustrated in Table V. The dependence of yield stress on magnetic field strength is characterized by utilizing the interpolated curve deduced out of the fluid contents obtained from the Lord Specification chart. A coil with multiple turns of wire is designated in the geometry as per American wire gauge (Brown & Sharpe) standards AWG 21.

**Table V. Materials Assigned For Respective Domains.**

Geometrical Domain	Designated Material
Piston, Piston shaft	AISI 4340
Cylinder	AISI 4340
Fluid	MRF 140 CG
Coil	Copper

The yield stress-magnetic field dependence curve and  $B-H$  curve for the selected fluid i.e. MRF 140 CG [15] are shown in figures 8 and 9 respectively.

**Fig. 8. Yield stress versus Magnetic field [15]**



**C. Mathematical model**

While using the MR damper as a controllable device, it is imperative that the preferred mathematical model is proficient enough to obtain the dynamic response of magneto-rheological fluid in order to examine its rheological characteristics precisely. Hence, it is crucial for the numerical model to accurately capture their non-linear feedback. Concerning Non-Newtonian fluids, Bingham model is one of the most basic models considered that can effectively predict their hysteretic behavior. One of the basic approximation underlying this model is that the fluid viscosity ( $\mu$ ) remains constant until considerable stress has been attained, causing the fluid to act predominantly as a quasi-solid rather than a viscous flowing liquid. When the field gets activated, MR fluid follows Bingham plastic model as per the following equation:

$$\tau = \tau_y(H) + \eta\dot{\gamma} \tag{4}$$

Where,  $\eta$  denotes the fluid’s apparent viscosity,  $\tau_y$  denotes the yield stress and  $\dot{\gamma}$  denotes shearing rate of the fluid. Two controlling factors which need to be given prime consideration are the viscosity and the minimum yield stress of MR fluid. The overall damping force resulting from

damper [1] is found out by adding the viscous and yield stress component which can be approximately stated as

$$F_d = F_\tau + F_\eta \quad (5)$$

$$= \left( 2.07 + \frac{12Q\eta}{12Q\eta + 0.4wh^2\tau_y} \right) \frac{\tau_y L A_p}{h} \text{sgn}(v)$$

$$+ \left( 1 + \frac{whv}{2Q} \right) \frac{12\eta Q L A_p}{wh^3} \quad (6)$$

Where,

$$Q = A_p \times v \quad (7)$$

$$A_p = \frac{\pi}{4} (D_p^2 - d_0^2) \quad (8)$$

Here,  $Q$  represents the volumetric discharge,  $A_p$  represents effective sectional-cut area of piston,  $D_p$  represents piston diameter,  $d_0$  is diameter of the piston shaft,  $v$  denotes the velocity of the piston,  $\tau_y$  is yield stress of the fluid,  $\eta$  denotes the fluid viscosity with zero magnetic field,  $L$  denotes the effective axial pole length,  $h$  denotes the fluid gap in between the piston and outer cylinder,  $w$  denotes the average perimeter of damper's circular flow path,  $\text{sgn}(v)$  for considering the reciprocation of the piston.

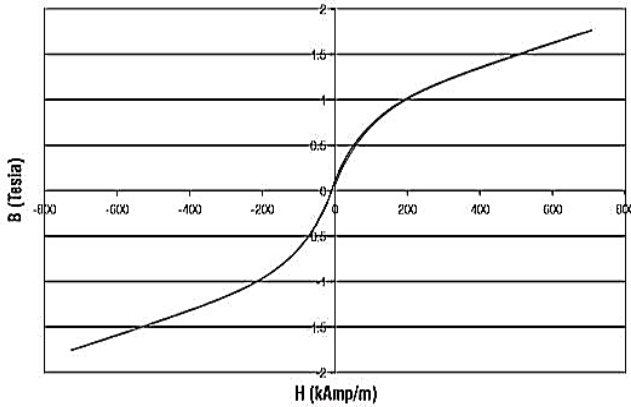


Fig. 9. B-H Curve [15]

### III. FINITE ELEMENT ANALYSIS

An axisymmetric geometry was established in COMSOL® Multiphysics package based on dimensions from Table IV with a view to assess the magnetic flux and field strength distribution of the proposed model. The MR damper consists of an electromagnetic coil which is placed at the piston head. An annular orifice of 0.7 mm is provided amidst the piston and the outer cylinder. The center axis of the piston rod accounts for the entire symmetry of the domain about that axis. Insulation is assumed around the entire perimeter of the domain so as to ensure there are no magnetic leakage across the boundary. The multi-turn coil is assumed to be of copper wire AWG 21 gauge diameter for 200 turns with a current varying from 0-2 Amperes given as an input to it. While carrying out static analysis in COMSOL®, DC current is given as an input to the simulating environment in the form of current density ( $J_e$ ) which is given by the following equation:

$$J_e = \frac{NI_{coil}}{A} e_{coil} \quad (9)$$

Where  $J_e$  is the current density,  $N$  is number of coil turns,  $I$  is the applied input current,  $A$  is the C.S.A. of coil and  $e_{coil}$  is the out-of-plane unit vector. AISI 4340 low alloy steel is used for both the piston and cylinder due to its high relative permeability. An MRF 140 CG is taken as the fluid for the proposed scheme with its properties based on graphs and values as recommended by the Lord Corp. Dependency of yield stress upon magnetic field intensity is characterized by making use of an interpolated graph generated from the corresponding material parameters available from the MR data sheet [15]. Physics considered is solved for stationary analysis using the Magnetic Fields sub-module of the AC/DC module. This particular sub-module comprehensively solves the well-known Maxwell's equations subjected to certain boundary conditions within its solver as given in [16]:

$$\nabla \times H = J + \frac{\partial D}{\partial t} \quad (10)$$

$$\nabla \times E = -\frac{\partial B}{\partial t} \quad (11)$$

$$\nabla \cdot D = \rho \quad (12)$$

$$\nabla \cdot B = 0 \quad (13)$$

Where,  $B$  denotes the magnetic flux density (in Tesla),  $D$  denotes the electric flux density (also called electric displacement) in (Coulombs per  $m^2$ ),  $E$  denotes the electric field intensity (in Volts per  $m$ ),  $H$  denotes the magnetic field intensity (in Amperes per  $m$ ),  $\rho$  denotes the volume charge density (in Coulombs per  $m^3$ ) and  $J$  denotes the current density (in Amperes per  $m^2$ ).

The FEA solver solves these equations in the corresponding electromagnetic domain for obtaining the values for magnetic flux density. Ampere's law is defined on the domain including the working gap. The laminar flow condition for the fluid is given as an input using the CFD module and is assigned over the domain of MR fluid gap. The design parameters and materials which are fed as an input in COMSOL® package in conjunction with the relevant physics necessary to solve the problem helps to attain the desired response in terms of magnetic flux density and field intensity which gives a clear insight as to how they are distributed in the domain of the proposed model.

### IV. DYNAMIC ANALYSIS OF MR DAMPER

The quarter-car model depicted in figure 10 is generally used for analyzing the suspension because it is quite elementary and is capable of acquiring the critical attributes of the full car model.

#### A. Mathematical modeling of a quarter-car model for an active suspension

To arrive at an equation where the vertical motions of a vehicle caused by the road irregularities are considered, this model is studied which assumes that motions due to road surface roughness are uniformly delivered to all wheels of a vehicle. The equations of motion are found with the help of Newton's 2<sup>nd</sup> law.



Unsprung mass generally refers to the mass of the suspension and wheels while the sprung mass refers to the mass of the body and other parts loaded on the suspension. The spring, shock absorber and a fluctuating force-generating component implanted amidst the sprung and unsprung masses comprise the entire suspension system. The equations of motion pertaining to figure 10 are given as:

$$m_s \ddot{z}_s + c_s(\dot{z}_s - \dot{z}_u) + k_s(z_s - z_u) = u_c \quad (14)$$

$$m_u \ddot{z}_u + c_s(\dot{z}_u - \dot{z}_s) + k_s(z_u - z_s) + c_u \dot{z}_u + k_u z_u = -u_c + k_u r + c_u \dot{r} \quad (15)$$

**B. Implementation in the Simulink environment**

The quarter car suspension model is integrated with the Bouc-Wen model and then the analysis is carried out numerically by virtue of modeling in MATLAB® Simulink. Although the identification of the non-linear hysteretic parameters is quite complicated and also necessitate for extensive experimental and numerical analyses for the purpose of acquiring pronounced gain of the MR damper attributes. The model proposed by Sulaymon L. Eshkabilov [17] created in MATLAB® Simulink environment is adopted for the purposed of simulation. The model created has two input variables viz.  $z_s$  and  $\dot{z}_s$  and one output parameter which is the force developed by the damper.

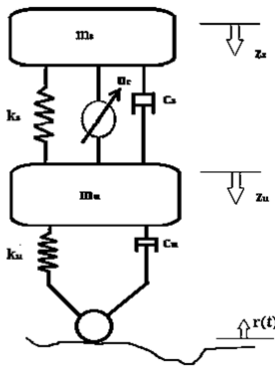


**Fig. 10. Quarter-car model.**

Here,  $z_s, \dot{z}_s$  and  $\ddot{z}_s$  represents the displacement, velocity and acceleration of sprung mass respectively,  $z_u, \dot{z}_u$  and  $\ddot{z}_u$  represents the displacement, velocity and acceleration of the unsprung mass (one half of axle mass and one wheel) respectively,  $c_s$  and  $c_u$  represents the damping coefficients of sprung (suspension) and unsprung (tyre) masses respectively,  $k_s$  and  $k_u$  are the spring stiffness of sprung and unsprung masses respectively,  $r(t)$  and  $\dot{r}$  denotes the road roughness disturbance and velocity w.r.t. longitudinal speed of the vehicle,  $u_c$  is the force developed by the controller (active damper).

**C. Identification of Bouc-Wen parameters**

In the model considered, road excitation is given as a sinusoidal wave of amplitude 75 mm (typically road disturbance height is taken as 0.075 m) with a frequency of 3.31 Hertz (angular frequency,  $\omega = 2\pi f = 20.8 \text{ rad s}^{-1}$ ). The sprung and unsprung masses of a typical hatchback commercial vehicle are taken as 475 and 45 kg respectively. Although the Bouc-Wen parameters  $\beta$  and  $\gamma$  pose no physical meaning, it greatly influences the contour of the hysteresis

curve. It is quite cumbersome to determine the exact values for the sake of determining the suitable trajectory of the loop. For the above model, the values are taken as  $\beta = 0.25$  and  $\gamma = 0.75$ . The value of constant n in the equation is taken as 2.0 as this parameter decides the slope of the curve as the system under consideration transforms between elastic and post-elastic loops. Larger values of n are restricted for this particular application as the model approaches the shape of a bilinear model. The sprung ( $k_s$ ) and unsprung ( $k_u$ ) stiffness of the vehicle are taken as 75000 and 260000  $N.m^{-1}$  respectively. Also, the sprung ( $c_s$ ) and unsprung ( $c_u$ ) damping coefficients are taken as 1433 and 14070  $Ns m^{-1}$  respectively. The input voltage given to the model is 5 V.

**V. RESULTS AND DISCUSSION**

The magnetic flux density is found to be maximum at the interface of coil and piston which is due to the fact that piston is made of steel which has very high permeability value. Property of high permeability makes the metal to generate a high intensity of magnetic field keeping the hysteresis losses into account. The maximum value of flux density is found out to be 0.14T. The yield stress value of the fluid can be computed corresponding to the magnetic field from the data provided by the Lord Corporation. Magnetic field intensity distribution for the analogous flux density is illustrated in figure 11. The magnetic field generated interacts with the fluid across the orifice and shows the maximum magnetic field at the interface of the coil and fluid gap. The average magnetic field along the fluid gap is expressed in A/m. Corresponding magnetic field contour is illustrated in figure 12.

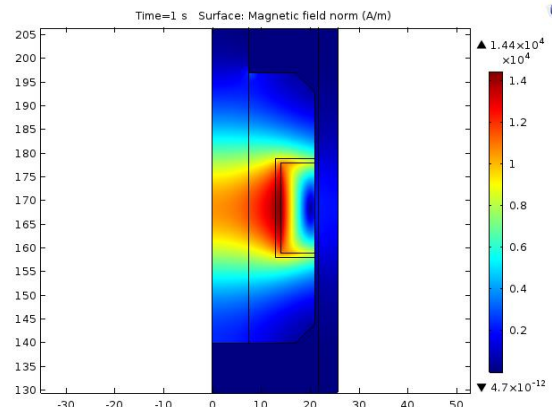


**Fig. 11. 2-D distribution of magnetic field intensity at 2 A**

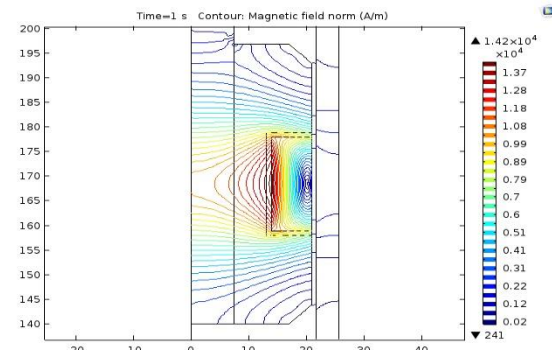


**Fig. 12. Magnetic field contour lines**

Thus, the maximum magnetic field intensity developed by the coil at an input current of 2 Amperes is found out to be  $1.44 \times 10^4 A/m$ . Corresponding yield stress developed on the fluid due to the effect of the magnetic field is found out from  $\tau_y - H$  curve and its value came to be  $8732.848 N.m^{-2}$ . Thus, on substituting the corresponding values in the damping force equation (6), the maximum damping force obtained from the proposed system is found out to be  $7402.61 N$ . For various increment in the current values, a time-dependent analysis is necessary for which current with respect to time is provided which yields the desired results. The variation in damping force for different values of current is displayed in Table VI. The damping force developed by the proposed damper for different values of current varying from 0.1 to 0.5 A with an increment of 0.1A is calculated. The corresponding plot is shown in figure 13.

**Table VI. Magnetic Field Strength Values For Corresponding Current Supplied.**

Current (in A)	Damping force (inN)
0.1	5257.44
0.2	5365.55
0.3	5424.79
0.4	5465.59
0.5	5506.39

A graph (figure 14) was plotted between flux density and fluid gap thickness for the sake of analyzing the extent of flux leakage occurring during the interaction of the generated flux with the fluid. It can be observed from the plot that as the thickness of the fluid gap increases, the flux leakage quantity also increases, thereby reducing the magnetic flux density.

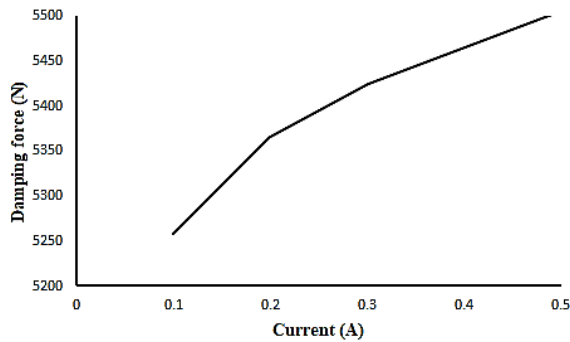


**Fig. 13. Plot Of Input Current With The Damping Force**

Also, variation of magnetic field intensity ( $H$ ) with the distance between poles ( $l$ ) is studied and analyzed. The plot between the two at different current levels is shown in figure 15. It is observed that as the distance between the poles increases, the magnetic field lines cease to flow between the poles, thereby reducing the field intensity. The hysteresis loop was plotted based on the dynamic conditions incorporating the Bouc-Wen hysteretic model and is depicted in figure 16.

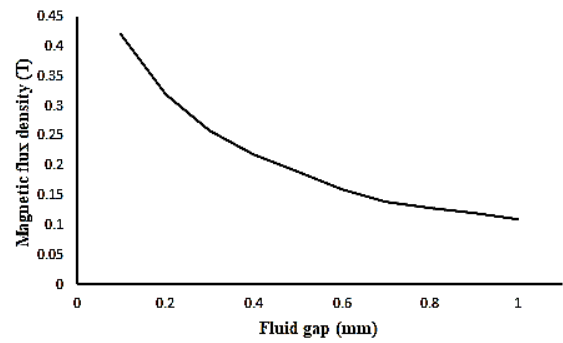


**Fig. 14. Flux Density Distribution Along The Fluid Gap**

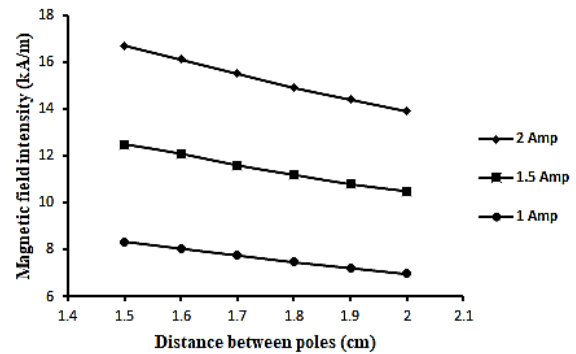


**Fig. 15. Plot Of Magnetic Field intensity versus Distance Between Poles**

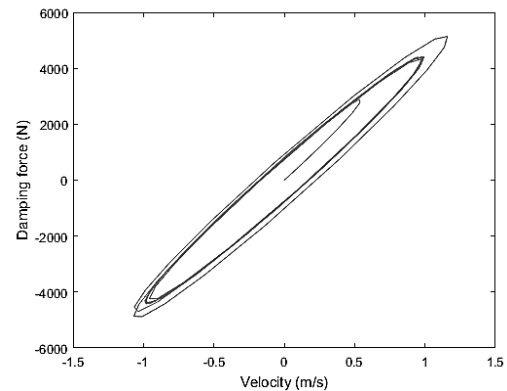


**Fig. 16. Damping Force Versus Velocity Plot**

From the loop generated, the maximum damping force is observed at  $5138.6 N$ . For a typical commercial vehicle of hatchback standard, the quarter car model parameters are taken as:

**Table VII. Quarter-car parameters for a conventional hatchback vehicle.**

Parameter	Values
Sprung mass ( $m_s$ )	475 kg
Unsprung mass ( $m_u$ )	45 kg
Suspension stiffness ( $k_s$ )	75000 N/m
Unsprung mass(tyre) stiffness ( $k_u$ )	260000 N/m
Sprung mass damping coefficient ( $c_s$ )	1433 Ns/m
Unsprung mass damping coefficient ( $c_u$ )	14070 Ns/m

Considering the data from Table VII, the maximum force is evaluated as  $8430.95 N$ .



**Table VIII. Comparison of damping forces between Bingham and Bouc-Wen model**

Model	Bingham model	Bouc-Wen model	Conventional damper
Maximum damping force generated (N)	7402.61	5138.60	8430.95

As deduced from Table VIII, the force generated by the proposed model is able to achieve 87.8% of the conventional damping force.

## VI. CONCLUSION

In this paper, two models are considered for the analysis viz. Bingham and Bouc-Wen model. For a vehicle in motion, the dampers are subjected to dynamic loading. Hence, it is essential to perform a dynamic analysis of the designed model. A substantial amount of damping is achieved in the proposed model when compared with the conventional damping force. However, for Bouc-Wen model, the damping forces comes out to be lower than the linear Bingham model due to the dynamic and hysteretic losses suffered by the damper. Even so, the Bouc-Wen model is smart enough to capture the exact non-linear hysteretic effects more precisely. Hence, it is imperative to determine more precise parameters of the Bouc-Wen model by virtue of experimental setup in order to enhance the damping characteristics. Also, keeping in view of the dimensional constraints, the design proposed is able to successfully replace the conventional dampers for the hatchback segment of commercial vehicles.

## REFERENCES

1. S.K. Mangal and Ashwani Kumar, "Experimental and numerical studies of magneto-rheological (MR) damper", Chinese Journal of Engineering, vol. 2014, doi:10.1155/2014/915694, 7 pages.
2. S.K. Mangal and Ashwani Kumar, "Geometric parameter optimization of magneto-rheological damper using design of experiment technique", International Journal of Mechanical and Materials Engineering Springer Open Journal, 2015, 10:4 DOI 10.1186/s40712-015-0031-1.
3. Krishnan Unni R. and Tamilarasan N., "Design and analysis of a magneto-rheological damper for an all-terrain vehicle", IOP Conf. Series: Materials Science and Engineering, 2018 310 012128 doi:10.1088/1757-899X/310/1/012128.
4. Luckachan K George, Tamilarasan N. and Thirumalini S., "Design and analysis of magneto rheological fluid brake for an all-terrain vehicle", IOP Conf. Series: Materials Science and Engineering, 2018 310 012127 doi:10.1088/1757-899X/310/1/012127.
5. M. Zapateiro, N. Luo, J. Rodellar and A. Rodriguez, "Modeling and Identification of Hysteretic Dynamics of MR Dampers and Application to Semiactive Vibration Control of Smart Structures", October 12-17, The 14th World Conference on Earthquake Engineering, 2018, Beijing, China.
6. N.M. Kwok, Q.P. Ha, M.T. Nguyen, J. Li and B. Samali, "Bouc-Wen model parameter identification for a MR fluid damper using computationally efficient GA", ISA Transactions, Volume 46, Issue 2, April 2007, pp. 167-179.
7. M. Giuclea, T. Sireteanu, D. Stanciou and C.W. Stammers, "Model parameter identification of vehicle vibration control with magnetorheological dampers using computational intelligent methods", Proceedings of the Institution of Mechanical Engineers. Part I: Journal of Systems and Control Engineering 218:569-81, 2004.
8. J. Rabinow, "The Magnetic Fluid Clutch", Transactions of the American Institute of Electrical Engineers, Jan. 1948, vol. 67, no. 2, doi: 10.1109/T-AIEE.1948.5059821, pp.1308-1315.
9. M.R. Jolly, J.W. Bender and J.D. Carlson, "Properties and Applications of Commercial Magnetorheological Fluids", SPIE 5th

- Annual Symposium on Smart Structures and Materials, San Diego, CA, March 1998.
10. J. Wang and G. Meng, "Magnetorheological fluid devices: principles, characteristics and applications in mechanical engineering", SAGE, Proceedings of the Institution of Mechanical Engineers, Vol 215, Part L, 2001.
11. R. Stanway, J.L. Sproston and N.G. Stevens, "Non-linear modeling of an electrorheological vibration damper", J. Electrosta., 1987.
12. R. Bouc, "Forced vibration of mechanical systems with hysteresis", Proceedings of the Fourth Conference on Non-linear oscillation, Prague, Czechoslovakia, 1967.
13. Y.K. Wen, "Method for Random Vibration of Hysteretic Systems", ASCE J. Engg. Mech. Div. 102(EM2), pp. 249-63, 1976.
14. B.F. Spencer, S.J. Dyke, M.K. Sain and J.D. Carlson, "Phenomenological model of a magnetorheological damper", ASCE J. Eng. Mech. 123 230-8, 1997.
15. LORD Corporation. Lord Technical Data, MRF-140CG Magneto-Rheological Fluid. Cary, NC, USA; 2008.
16. Comsol AB, 'AC/DC Module users guide', Comsol Documentation, ver. 5.0, pp. 28-30, 2015.
17. Sulaymon L. Eshkabilov, "Modeling and Simulation of Non-Linear and Hysteresis Behavior of Magneto-Rheological Dampers in the Example of Quarter-Car Model", International Journal of Theoretical and Applied Mathematics. Vol. 2, No. 2, doi: 10.11648/j.ijtam.20160202.32, 2016, pp. 170-189.

## AUTHORS PROFILE



**Rupesh Kumar Patnaik**  
M.Tech (Automotive Engg.),  
Department of Mechanical Engineering,  
Amrita School of Engineering, Coimbatore



**N Tamilarasan**  
M.Tech, Assistant Professor,  
Department of Mechanical Engineering,  
Amrita School of Engineering, Coimbatore